

Structure–Activity Correlation in Titanium Single-Site Olefin Polymerization Catalysts Containing Mixed Cyclopentadienyl/Aryloxy Ligand

Thomas A. Manz,[†] Khamphree Phomphrai,[‡] Grigori Medvedev,[†] Balachandra B. Krishnamurthy,[†] Shalini Sharma,[‡] Jesmin Haq,[†] Krista A. Novstrup,[†] Kendall T. Thomson,[†] W. Nicholas Delgass,[†] James M. Caruthers,^{*,†} and Mahdi M. Abu-Omar^{*,‡}

School of Chemical Engineering and Department of Chemistry, Purdue University, West Lafayette, Indiana 47907

Received June 9, 2006; E-mail: caruther@ecn.purdue.edu; mabuomar@purdue.edu

Single-site polymerization catalysts are commercially important because the polymer's molecular architecture can be varied by changing the catalyst structure.¹ Ti and Zr mixed cyclopentadienyl aryloxy complexes have recently received considerable interest as olefin polymerization catalysts.² A catalyst structure library can be created by varying the substituents on the cyclopentadienyl and aryloxy ligands, where the catalyst's performance depends on the nature of the ligands.

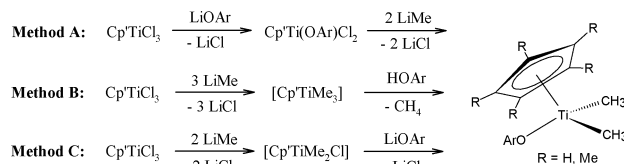
We report the synthesis of eighteen titanium cyclopentadienyl aryloxy complexes and their propagation rate constants for 1-hexene polymerization. A correlation between k_p and the catalyst structures is developed using DFT-computed ligand cone angles and ion pair separation energies (E_{IPS}). This correlation takes the form of an Arrhenius-like relationship, where the pre-exponential factor (k_0) is correlated to the ligand cone angles and the activation energy term (E_a) is correlated to E_{IPS} .

A series of compounds $\text{Cp}'\text{Ti}(\text{OAr})\text{Me}_2$, where $\text{Cp}' = \text{C}_5\text{H}_5$ (Cp) or C_5Me_5 (Cp^*) were synthesized from three general routes (Scheme 1). For very bulky aryloxides such as $\text{OC}_6\text{H}-2,3,5,6\text{-Ph}_4$, a simple deprotonation by $\text{Cp}'\text{TiMe}_3$ failed. The easiest way to incorporate bulky aryloxides was from the reaction of $\text{Cp}'\text{TiCl}_3$ and LiOAr followed by complete methylation (method A). For moderately bulky aryloxides such as $\text{OC}_6\text{H}_3-2,6\text{-R}_2$ ($\text{R} = \text{Me, Et, }^i\text{Pr}$), the reaction of $\text{Cp}'\text{TiCl}_3$ and LiOAr in method A yielded a mixture of mono- and bis(aryloxy) titanium complexes. The most effective preparation of this type of catalyst was from deprotonation of the parent phenol with $\text{Cp}'\text{TiMe}_3$ at low temperature (method B). For less bulky aryloxides having no ortho substituents, the formation of the bis(aryloxy) byproduct became problematic in methods A and B. The solution was to react $\text{Cp}'\text{TiMe}_2\text{Cl}$ with LiOAr to exclude the possibility of bis(aryloxy) complex formation (method C).³

The addition of 1 equiv $\text{B}(\text{C}_6\text{F}_5)_3$ to $\text{Cp}'\text{Ti}(\text{OAr})\text{Me}_2$ in toluene immediately gave thermally unstable contact ion pairs $[\text{Cp}'\text{Ti}(\text{OAr})\text{Me}]^+[\text{MeB}(\text{C}_6\text{F}_5)_3]^-$ that were active for the polymerization of 1-hexene. Polymerization reactions were followed by ¹H NMR at 0 °C, and polymer molecular weights were determined by GPC analysis. A kinetic model containing initiation, propagation, and deactivation steps was fit to the $\ln([1\text{-hexene}]/[1\text{-hexene}]_0)$ versus time concentration profiles and M_n data to obtain the k_p values (Table 1). The model equations and fitted kinetic profiles are presented in the Supporting Information.

In chain propagation, the monomer first coordinates to the metal to form a π -complex and then inserts to extend the polymer chain.^{1e} The chemical structure of the counterion is known to have a large effect on the catalyst's activity, and it has generally been established that weakly coordinating counterions are needed to achieve high polymerization rates.^{1a,b} Detailed experiments can be used to extract the rate constants for the different reaction steps.^{1d,f}

Scheme 1. Catalyst Precursor Synthesis



Our structure–activity correlation is based on the idea that partial displacement of the counterion from the metal center to allow space for monomer coordination and insertion is a key factor affecting the polymerization rate. On the basis of this idea, the reaction rate should increase when separation of the counterion is easier and when the metal center is less sterically hindered, because these two factors increase monomer access to the metal. Ion pair separation energies (E_{IPS}) and ligand cone angles were selected as quantitative descriptors of these two factors. E_{IPS} was calculated by subtracting the DFT-computed SCF energy of the contact ion pair from that of the bare cation $[\text{Cp}'\text{Ti}(\text{OAr})\text{Me}]^+$ and counterion $[\text{MeB}(\text{C}_6\text{F}_5)_3]^-$ in a toluene-like solvent. The ligand cone angle was defined as the largest $\text{X}-\text{M}-\text{Y}$ angle where M is the center of the metal atom and X and Y are two points on the van der Waals surface of the ligand outside the metal's van der Waals sphere.⁴ Using the DFT optimized contact ion pair geometries, this definition provided the ligand steric descriptors $\theta_{\text{Cp}'}$ and θ_{OAr} .

In Gaussian 03,⁵ the OLYP/6-311++G** method was chosen because of its high accuracy and much lower computational cost than hybrid methods like B3LYP.⁶ Vacuum and PCM-optimized geometries for the ion pair of catalyst 1 were computed and found to be nearly identical. As PCM geometry optimization was very costly, all geometries were optimized in vacuum. The PCM model was then used to compute solvation energies on these geometries.³

The solid angle subtended by cone angle θ equals $4\pi \sin^2(\theta/4)$. Thus, the solid angle $4\pi\gamma$ available for monomer approach to the Ti site when the counterion is partially displaced is approximated by

$$\gamma = 1 - \sin^2(\theta_{\text{Cp}'}/4) - \sin^2(\theta_{\text{OAr}}/4) - f \quad (1)$$

where f is a factor that accounts for ligand orientation and space blocked by the growing chain and partially displaced counterion. The experimental data is fit to a correlation in the form of an Arrhenius-like relationship:

$$k_{\text{pred}} = k_0 e^{-E_a/RT} = \gamma a_0 e^{-E_0/RT} e^{-\alpha E_{\text{IPS}}/RT} \quad (2)$$

where k_{pred} is the predicted value of k_p , R is the gas constant, T is absolute temperature, and a_0 , E_0 , and α are model parameters.

Figure 1 shows the experimental k_p plotted as a function of E_{IPS} and divided into different catalyst families where the smaller E_{IPS} was used for catalysts 13, 15, and 17. Family A contains the Cp catalysts, while the Cp^* catalysts are divided as (B) no methoxy, coordinating,

[†] School of Chemical Engineering.

[‡] Department of Chemistry.

Table 1. Summary of Experimental and Computed Parameters for $[\text{Cp}^*\text{Ti}(\text{OAr})\text{Me}]^+[\text{MeB}(\text{C}_6\text{F}_5)_3]^-$ Catalysts

catalyst	Cp' ligand	OAr ligand	family	k_p ($\text{M}^{-1}\text{s}^{-1}$)	M_n (g/mol)	θ_{Cp} (deg)	θ_{OAr} (deg)	E_{IPS} (kcal/mol)
1	Cp	$\text{OC}_6\text{H}_2\text{-2,6-Me}_2\text{-4-Br}$	A	0.22	3200	126.3	127.5	35.7
2	Cp	$\text{OC}_6\text{H}_3\text{-2,6-Et}_2$	A	0.34	5200	127.3	131.7	34.6
3	Cp	$\text{OC}_6\text{H}_3\text{-2,6-}^i\text{Pr}_2$	A	0.42	6200	127.5	137.2	34.1
4	Cp*	OC_6H_5	B	0.42	4500	153.8	94.9	31.4
5	Cp*	$\text{OC}_6\text{H}_4\text{-4-F}$	B	0.27	4700	154.7	94.8	32.1
6	Cp*	$\text{OC}_6\text{H}_4\text{-4-Cl}$	B	0.24	5200	154.9	94.6	32.1
7	Cp*	$\text{OC}_6\text{H}_4\text{-4-Br}$	B	0.26	5200	154.6	94.6	31.8
8	Cp*	$\text{OC}_6\text{H}_4\text{-4-Ph}$	B	0.38	4800	154.5	94.6	31.2
9	Cp*	$\text{OC}_6\text{H}_4\text{-4-}^i\text{Bu}$	B	0.48	5100	154.8	94.5	31.0
10	Cp*	$\text{OC}_6\text{H}_3\text{-2,6-Me}_2$	C	0.51	28500	153.1	126.3	28.9
11	Cp*	$\text{OC}_6\text{H}_3\text{-2,6-Et}_2$	C	0.78	44700	153.5	131.3	28.4
12	Cp*	$\text{OC}_6\text{H}_3\text{-2,6-}^i\text{Pr}_2$	C	0.92	62300	153.3	135.7	26.6
13	Cp*	$\text{OC}_6\text{H}_4\text{-2-(cyclohexyl)}$	B	0.74	17200	154.4	125.8	30.2 (d), 30.9 (p) ^a
14	Cp*	$\text{OC}_6\text{H}_2\text{-2,6-Me}_2\text{-4-Br}$	C	0.28	27900	153.7	126.2	29.6
15	Cp*	$\text{OC}_6\text{H}_4\text{-2-(CH}_2\text{Ph)}$	D	0.27	14400	153.6	111.9	23.9 (d), 31.1 (p) ^a
16	Cp*	$\text{OC}_6\text{H}_2\text{-2,3,5,6-Ph}_4$	D	1.36	9500	152.9	162.7	14.1
17	Cp*	$\text{OC}_6\text{H}_4\text{-3-(OMe)}$	E	0.25	3100	154.7	94.6	30.7 (d), 31.1 (p) ^a
18	Cp*	$\text{OC}_6\text{H}_4\text{-4-(OMe)}$	E	0.20	5400	154.6	95.0	30.2

^a For aryloxide ligands with only one ortho or meta substituent group, the substituent group can be either distal (d) or proximal (p) to the growing chain.

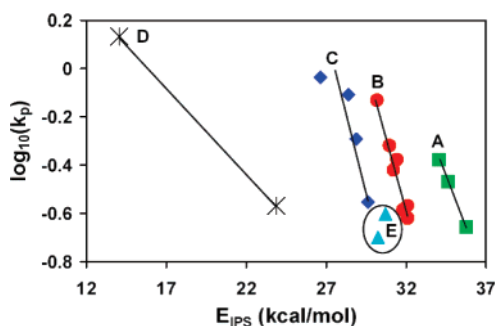


Figure 1. Experimental 1-hexene polymerization rate constants (k_p) versus computed ion pair separation energies in toluene (E_{IPS}).

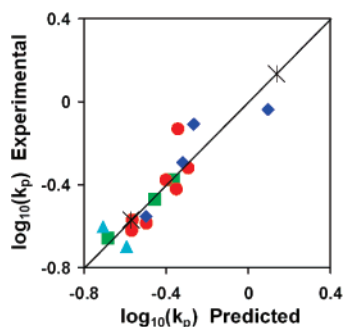


Figure 2. Prediction of the propagation rate using eqs 1 and 2 with $\alpha = 0.300$, $f = 0.187$, and the following values of A ($\text{M}^{-1}\text{s}^{-1}$) according to the indicated catalyst family: A, 3.01×10^8 (green square); B, 5.22×10^7 (red circle); C, 2.65×10^7 (blue diamond); D, 6.88×10^5 (crossed lines); and E, 1.77×10^7 (green triangle).

or 6 substituents; (C) alkyl substituents in both 2, 6 positions; (D) substituent phenyl rings that partially coordinate to the Ti center in the bare cation; and (E) methoxy substituents. Catalyst 13 is included in family B because in the state with lower E_{IPS} (distal conformation) the cyclohexyl group points away from the growing chain providing negligible steric hindrance. A linear correlation between $\log(k_p)$ and E_{IPS} emerges for each catalyst family. The methoxy catalysts (family E) are structurally similar to family B but have lower k_p values for comparable E_{IPS} . This could potentially be caused by a coordination between methoxy groups and either a second Ti center or the $\text{B}(\text{C}_6\text{F}_5)_3$ activator, since both of these are prone to bind ethers.

The experimental data were fit to eqs 1 and 2 by minimizing the sum of $(\log(k_p) - \log(k_{\text{pred}}))^2$. Since the experimental data were

collected at the same temperature, a single parameter $A = a_0 e^{-E_0/RT}$ was used for each catalyst family. The correlation provides a good fit to the experimental data (Figure 2), suggesting its underlying physical basis is correct. This means a portion of E_a for chain propagation is due to separation of the ion pair. Because the ion pair only separates to a finite distance, only part of E_{IPS} contributes to E_a and thus $0 < \alpha < 1$. The correlation also shows that steric factors are important and can be approximately described in terms of ligand cone angles. Other physical factors which are not explicitly accounted for are implicitly grouped into different A's for different catalyst families. We are now studying how these additional factors relate to catalyst structure with the goal of developing a more comprehensive predictive model.

Acknowledgment. Financial support was provided by the U.S. Department of Energy Catalysis Science Grant No. DE-FG-0203ER15466. Supercomputing resources were provided by Information Technology at Purdue and the National Center for Supercomputing Applications, Grant No. MCA04N010.

Supporting Information Available: Complete ref 5; experimental details, kinetic and error analysis, and model optimization; DFT geometries and solvation calculations; X-ray crystal structure for $\text{Cp}^*\text{Ti}(\text{OC}_6\text{H}_2\text{-2,3,5,6-Ph}_4)\text{Me}_2$. This material is available free of charge via the Internet at <http://pubs.acs.org>.

References

- (1) (a) Chen, M. C.; Roberts, J. A. S.; Marks, T. J. *J. Am. Chem. Soc.* **2004**, *126*, 4605–4625. (b) Chen, E. Y.-X.; Marks, T. J. *Chem. Rev.* **2000**, *100*, 1391–1434. (c) *Chem. Rev.* **2000**, *100* (4). (d) Veghini, D.; Henling, L. M.; Burkhardt, T. J.; Bercaw, J. E. *J. Am. Chem. Soc.* **1999**, *121*, 564–573. (e) Lanza, G.; Fragala, I. L.; Marks, T. J. *Organometallics* **2002**, *21*, 5594–5612. (f) Liu, Z.; Somsook, E.; White, C. B.; Rosaaen, K. A.; Landis, C. R. *J. Am. Chem. Soc.* **2001**, *123*, 11193–11207.
- (2) (a) Byun, D. J.; Fudo, A.; Tanaka, A.; Fujiki, M.; Nomura, K.; Nomura, M. *Macromolecules* **2004**, *37*, 5520–5530. (b) Nomura, K.; Tsubota, M.; Fujiki, M. *Macromolecules* **2003**, *36*, 3797–3799. (c) Nomura, K.; Fudo, A. *J. Mol. Catal. A: Chem.* **2004**, *209*, 9–17. (d) Nomura, K.; Itagaki, K.; Fujiki, M. *Macromolecules* **2005**, *38*, 2053–2055. (e) Wang, W.; Fujiki, M.; Nomura, K. *J. Am. Chem. Soc.* **2005**, *127*, 4582–4583. (f) Fenwick, A. E.; Phomphrai, K.; Thorn, M. G.; Vilardo, J. S.; Trefun, C. A.; Hanna, B.; Fanwick, P. E.; Rothwell, I. P. *Organometallics* **2004**, *23*, 2146–2156. (g) Phomphrai, K.; Fenwick, A. E.; Sharma, S.; Fanwick, P. E.; Caruthers, J. M.; Delgass, W. N.; Abu-Omar, M. M.; Rothwell, I. P. *Organometallics* **2006**, *25*, 214–220.
- (3) See Supporting Information for details.
- (4) Tolman, C. A. *J. Am. Chem. Soc.* **1970**, *92*, 2956–2965.
- (5) Frisch, M. J.; et al. *Gaussian 03*; Gaussian Inc.: Pittsburgh, PA, 2003.
- (6) Baker, J.; Pulay, P. *J. Chem. Phys.* **2002**, *117*, 1441–1449.

JA0640849